

PACS numbers: 52.35.Tc; 62.50.Ef; 42.55.Lt
DOI: 10.1070/QE2011v041n10ABEH014572

Criteria for formation of low-frequency sound under wide-aperture repetitively pulsed laser irradiation of solids

V.N. Tishchenko, V.G. Posukh, A.I. Gulidov, V.I. Zapryagaev, A.A. Pavlov, E.L. Boyarintsev, M.P. Golubev, I.N. Kavun, A.V. Melekhov, L.S. Golobokova, I.B. Miroshnichenko, Al.A. Pavlov, A.S. Shmakov

Abstract. **The criteria for merging shock waves formed by optical breakdowns on the surface of solids have been investigated. Targets made of different materials were successively irradiated by two CO_2-laser pulses with energies up to 200 J and a duration of $\sim$1 μs. It is shown that the criteria under consideration can be applied to different targets and irradiation regimes and make it possible to calculate the parameters of repetitively pulsed laser radiation that are necessary to generate low-frequency sound and ultrasound in air.**

Keywords: *laser radiation, optical breakdown, shock waves, sound, mechanism of wave merging, criteria, target.*

1. Introduction

Many studies have been devoted to the gas-dynamic and optoacoustic effects induced by optical breakdown (see, for example, [1–7]). Repetitively pulsed laser radiation with a high pulse repetition rate ($f \sim 100$ kHz) [8–10] opens new areas of laser applications: control of the supersonic streamline flow [11–13], laser engines [14], laser-plasma technologies [15], and generation of low-frequency sound and ultrasound [16]. These new possibilities stem from the fact that the peak power exceeds the average power by a factor of $\sim$100; the properties of optical pulsating discharge that is formed in the focus of the beams; and the mechanism of merging of the shock waves [17–19] formed by laser sparks. The discharge burns in an immobile gas, in a flow, or in a focus moving at a velocity of $\sim$300 m s^{-1} [8, 12, 18–21]. The essence of shock wave merging (SWM) is as follows: when merging, shock waves (SWs) form a low-frequency wave; the duration of the compression phase of this wave depends linearly on the number of laser pulses in the train and, accordingly, on the total energy spent, whereas, in the case of single spark (explosion), the duration of the compression phase depends weakly on the pulse energy Q ($\propto Q^{1/6}$) [22]. Shock wave merging occurs in gases and plasma with a magnetic field [23] under certain conditions (i.e., when certain criteria are satisfied). Shock waves merge on the scale of the spark dynamic radius and may take away up to $\sim$20% of laser-pulse energy [18, 24].

The pulsating optical discharge formed by trains of laser pulses generates ultrasound at the pulse repetition rate in the trains, $f \sim 10-100$ kHz, and low-frequency sound at the train repetition rate F [16, 18]. The SWM effect is enhanced with an increase in f or the pulse energy; in this case, the fraction of the sound power at the frequency F also increases and may greatly exceed that under amplitude modulation, where the corresponding dependence is reverse (the power fraction is proportional to $1/f$). If the SWM effect is weak, the spectrum corresponds to the amplitude modulation. The distance at which sound is generated in air is limited by the optical breakdown threshold ($\sim$2 GW cm^{-2}). Remote generation of sound can be implemented under irradiation of dense targets, for which the threshold is reduced by a factor of $\sim$100 [2]. At a large distance the light spot diameter may exceed the length of the breakdown region h ($h \approx 1$ cm); this situation corresponds to planar breakdown.

The purpose of this study was to find the criteria of SWM manifestation in targets exposed to wide-aperture laser radiation. The applicability of these criteria was verified experimentally [17, 18] for targets made of different materials in a wide range of irradiation conditions (light-spot areas S, pulse energies Q, and energy densities $q = Q/S$).

In our experiments a target was successively irradiated by two CO_2-laser pulses. This is insufficient for studying the plasma effects near targets but applicable for determining the merging criteria: if the first SWs merge, the next SWs will merge as well. Limitations on the number of pulses were revealed neither in our calculations (see, for example, [25]) nor in the experiments (similar to those [18–20]) with a large number of pulses (the average power was $\sim$1.5 kW). The criteria were checked by varying the radiation parameters. Nonoptimal versions, which modelled the effect of screening the radiation and SWs by the laser plume at a large number of pulses, were also considered. For example, at q values close to the breakdown threshold, the structure of the laser plasma is significantly inhomogeneous. At $q \sim 20-50$ J cm^{-2} the plume near the target and the breakdowns at air aerosol and target particles may affect the formation of SWs and their merging. SW merging was hindered by the difference in the light-spot areas.

The experiments were performed for metals and insulators with different properties. Silver has a high thermal conductivity and a maximum reflectance for laser radiation, the corresponding properties of titanium are low, and the steel parameters have intermediate values. Window glass (inorganic matter) is characterised by a high melting temperature and radiation

V.N. Tishchenko, V.G. Posukh, E.L. Boyarintsev, A.V. Melekhov, L.S. Golobokova, I.B. Miroshnichenko Institute of Laser Physics, Siberian Branch, Russian Academy of Sciences, prosp. Akad. Lavrent'eva 13/3, 630090 Novosibirsk, Russia;
e-mail: tvn25@ngs.ru;
A.I. Gulidov, V.I. Zapryagaev, A.A. Pavlov, M.P. Golubev, I.N. Kavun, Al.A. Pavlov, A.S. Shmakov S.A. Khristianovich Institute of Theoretical and Applied Mechanics, Siberian Branch, Russian Academy of Sciences, ul. Institutskaya 4/1, 630090 Novosibirsk, Russia;

Received 24 February 2011; revision received 1 August 2011
Kvantovaya Elektronika **41** (10) 895–900 (2011)
Translated by Yu.P. Sin'kov

absorption in a thin surface layer. Caprolon and Plexiglas (organic materials) differ by a larger radiation-absorption depth and low evaporation energy.

We investigated the applicability of the criteria for SWM, which were obtained for an optical pulsating discharge in a gas. In the case of immobile discharge, the criteria for the dimensionless repetition frequency of laser pulses,

$$\omega = fR_3/c_0 \tag{1}$$

were as follows [17, 18]. At

$$\omega < \omega_1 \approx 0.7 \tag{2a}$$

SWs do not interact; at

$$\omega > \omega_2 \approx 5.8 \tag{2b}$$

the SW compression phases merge partially to generate a low-frequency wave; and at

$$\omega_1 < \omega < \omega_2 \tag{2c}$$

there is a transition region. The frequencies

$$\omega > 1.5\omega_2 \tag{2d}$$

are not energetically efficient: the front of the subsequent SW comes up with the front of the previous SW, due to which the pressure increases and the compression-phase duration of the resulting wave changes only slightly. In (1) and (2) c_0 is the speed of sound in the gas; $R_3 = (b\delta Q/p_0)^{1/3}$ (R_3, Q, and p_0 are measured in m, J, and Pa, respectively) or $R_3 = 2.15(b\delta Q/p_0)^{1/3}$ (R_3, Q, and p_0 are in cm, J, and atm, respectively) is the dynamic radius; p_0 is the gas pressure; $\delta \approx 0.5-0.7$ is the pulse energy fraction absorbed in the plasma (it depends on the target material); and b is a geometric factor ($b = 2$ and 1 for the breakdowns on the target and in the gas, respectively).

Let us estimate the applicability conditions for the criteria. Some limitations are due to the efficient pulse energy conversion into the SW energy. For example, SWs are formed if the pressure jump in the plasma exceeds greatly the pressure of the medium where breakdown occurs. We will find the pulse-energy density from the condition that, at $p/p_0 > 10$ (p is the pressure in the SWs) SWs take away a significant part ($\eta \approx 1 - (p_0/p)^{(\gamma-1)/\gamma} \approx 0.3$) of the pulse energy [2]. Hence, $q = \delta^{-1}(p_0/p)(\gamma_0 - 1)\varepsilon_0 h/(\gamma - 1) \approx 5-10$ J cm^{-2}. Here, $\delta = 0.5$, $h = 0.5-1$ cm, ε_0 is the energy density in air (in J cm^{-3}), $\gamma_0 = 1.4$ is the adiabatic index for air, and $\gamma \sim 1.2$ is the adiabatic index for plasma. The optimal pulses are short ones (~200 ns), for which $\eta \approx 20\%$ can be reached at $q \sim 10$ J cm^{-2} [24]. The limiting value $q \sim 15-20$ J cm^{-2} is due to the breakdown at aerosol in air [7]. Taking into account the weak dependence $\omega \propto R_3 \propto \delta^{1/3}$, one can assume that $\delta \approx 1$; this assumption simplifies the use of the criteria.

Let us estimate the maximum values of the light-spot diameter D_3, the pulse energy, and the other parameters, at which criteria (2) are valid. It follows from the experiments that D_3 satisfies the condition $D_3 \approx 2R_3$. At a distance from the spot centre larger than R_3, the SW is hemispherical. The radius R_3 can be calculated based on the assumption that the energy $Q_3 = q\pi D_3^2/4$, which is absorbed during breakdown, is concentrated in the centre of the irradiated area. Note that the SW compression phases are combined at a distance smaller than R_3, where SWs propagate with a supersonic velocity. Using the corresponding expression for R_3, we find the maximum values of the diameter $D_3 \approx 2\delta q/p_0$ and the pulse energy $Q_3 \approx \pi\delta^2 q^3/p_0^2$. Using (2), we obtain the maximum values of the average power in laser-pulse trains, $W_3 = fQ_3 = 0.79c_0\omega\delta q^2/p_0 = 2.7\times10^4\omega\delta q^2/p_0$, and the pulse repetition rate $f = 0.25\times c_0\omega p_0/(\delta q) = 8.55\times10^3\omega p_0/(\delta q)$. Here, $c_0 = 3.4\times10^4$ cm s^{-1}. For $q = 5$ J cm^{-2}, $p_0 = 1$ atm, and $\omega = 5$, we have $D_3 < 10$ cm, $Q_3 = 393$ J, $W_3 = 3.38\times10^6$ W, and $f = 8.55\times10^3$ Hz. Relation (2) can be used to find the radiation parameters for different (including high-power) lasers.

2. Experimental

We studied experimentally the applicability of criteria (2) to targets made of different materials and irradiated under different conditions and considered the effect of the following factors on the SWs and criteria: the energy density q, the light-spot areas on the target for the first (S_1) and second (S_2) beams, and the plume of breakdowns at the target and at air aerosol and target particles. The schematic of the experiments is shown in Fig. 1. The target was located in air and irradiated by two pulses with the delay $t_d \approx 0-3$ ms. The width of the CO_2 laser pulse was $t_r \sim 1$ μs. The beams were aligned and directed upward along to the normal to the target centre. The radiation was focused by a lens with a focal length of 120 cm. The target was suspended on thin wires between the lens and its focal plane. The pulse energy ($Q = 20-250$ J) was varied by attenuators, the light-spot areas on the target ($S = 2.5-38$ cm^2) were changed by displacing the target with respect to the waist, and the energy density was $q = Q/S \approx 2-50$ J cm^{-2}. The targets were shaped as disks 50 cm in diameter, a value exceeding R_3 by a factor of 2–5; the target size affected the SWs only slightly. The frequency ω was varied by changing the energy of the second pulse, Q_2, and its delay, t_d. In the repetitively pulsed regime $t_d = 1/f$. Expression (1) can be written in the form $\omega = 79Q_2^{1/3}/t_d$, which is convenient for analysing the data reported below. Here, Q_2 is in J and t_d is in μs.

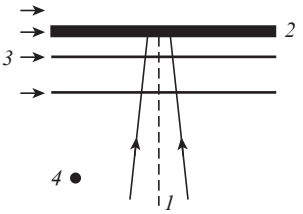

Figure 1. Schematic diagram of measurements: (*1*) laser beams, aligned on a (*2*) target 50 cm in diameter; (*3*) probe laser radiation, used for shadow diagnostics (the beam axis is displaced from the target surface); and (*4*) an SW pressure sensor in air.

The density gradients were visualised by a shadow method [21]. The probe laser wavelength was $\lambda = 0.63$ μm, and the exposure time was 2 μs. The optical-beam diameter was 15 cm, and its axis was displaced by ~6 cm from the target surface. The excess pressure in SWs, $P = p - p_0$, was measured by a sensor located at a distance of 27 cm from the centre of the irradiated spot and at 23 cm from the surface. The sensor was placed at this point because SW merging is completed at $R_3 \sim 10-15$ cm, and the profile of the resulting SW does not change.

Figure 2 presents shadow photographs and pressure-sensor readings for the SWs generated during irradiation of Plexiglas.

The radiation energy density ($q \approx 5$ J cm^{-2}) exceeds the breakdown threshold by a factor of ~1.5. Here, the criteria are illustrated by the example of nonoptimal irradiation mode: the optical breakdown is nonuniform over the beam cross section, and the ratio of the SW energy to the pulse energy is smaller than at $q > 10$ J cm^{-2} by a factor of ~2. The beam axis passes through the cavity centre. It can be seen in Fig. 2a that at $\omega = 2.6$ the front of the second SW is located in the low-pressure phase of the first SW. With an increase in the frequency ω, the SW compression phases partially merge to generate a SW, the length of which exceeds that of the SW formed by one pulse by a factor of almost 2 (Fig. 2b). At $\omega > 1.5\omega_2$ the front of the second SW comes up with the front of the first SW (Fig. 2c); this situation is inappropriate for generating a low-frequency wave. The increase in P is related to the increase in q. Merging of SWs can be observed in shadow photographs (Fig. 2) by the position of their fronts. A cavity is formed during the plasma expansion near the target. The dark region

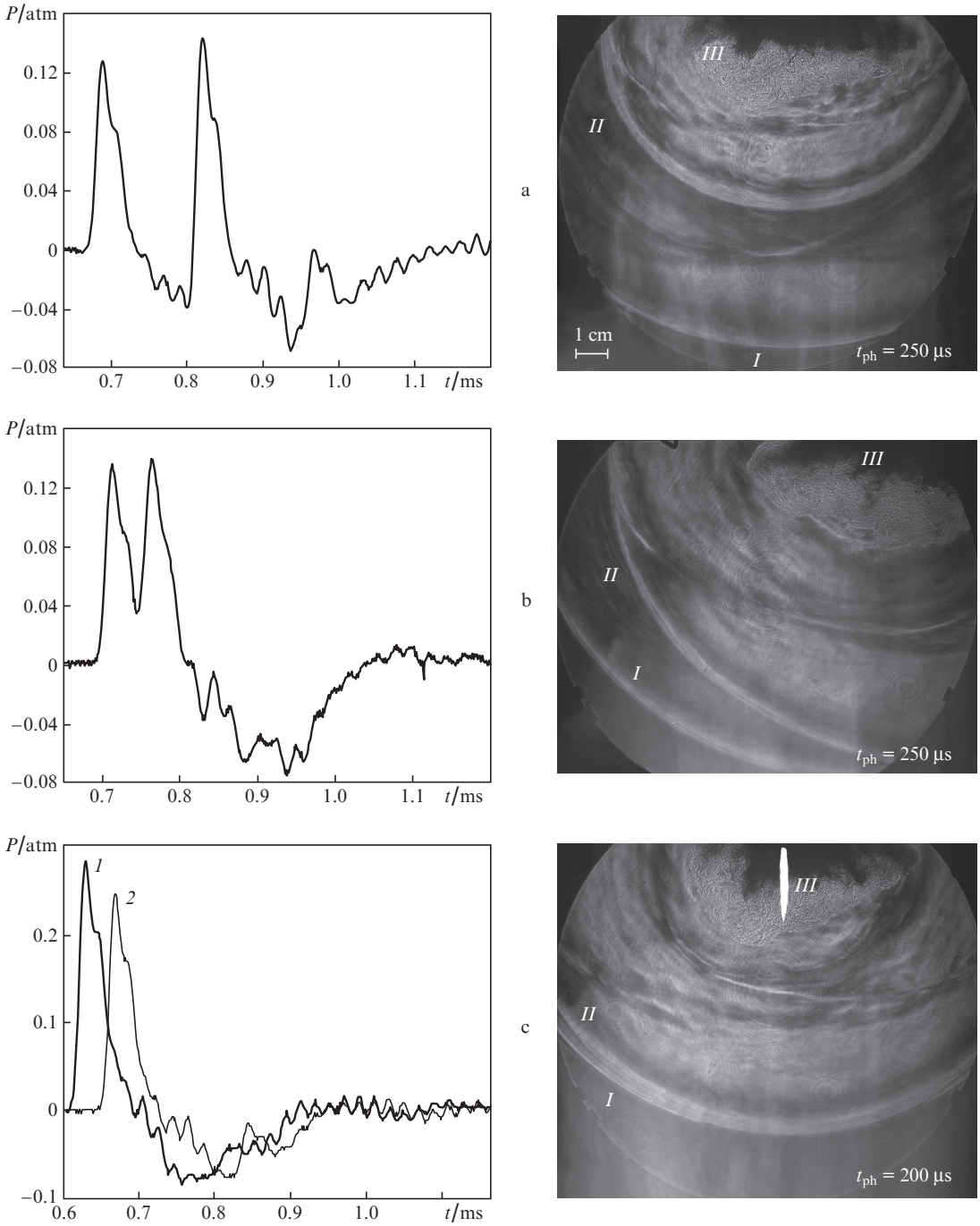

Figure 2. Time dependences of the pressure in SWs (left) and shadow photographs (right) for irradiation of a Plexiglas target [(*I*, *II*) the fronts of the first and second SWs and (*III*) the cavity]. The radiation is directed upward. The beam-irradiated areas are $S_1 = 38$ cm^2 and $S_2 = 22$ cm^2 and the optical field diameter in the photographs is 15 cm; t_{ph} is the time of shadow shot. The varied parameters are (a) $Q_1 = 183$ J, $Q_2 = 109$ J, $t_d = 150$ μs, and $\omega = 2.6$; (b) $Q_1 = 191$ J, $Q_2 = 121$ J, $t_d = 46$ μs, and $\omega = 8.7$; and (c) $Q_1 = (1)$ 191 and (2) 187 J, $Q_2 = (1)$ 116 and (2) 111 J, $t_d = (1)$ 2 and (2) 35 μs, and $\omega = (1)$ 197 and (2) 11. The shadow photograph in panel c corresponds to curve (2).

(opaque for the probe radiation) is a cloud of dense target vapour. The second-pulse breakdown occurs on the target surface and in its vapour. The shadow photographs suggest that at $t = 0-200$ μs the average velocity of the cavity boundary is ~ 100 m s^{-1}.

At $q > 10$ J cm^{-2} a flash of Plexiglas vapour was observed at a distance of few centimetres from the target. The luminescence delay of 2–5 ms with respect to the irradiation instant is due to the mixing of vapour with air. The cloud was ~30 cm in size, and the luminescence time was 5–20 ms. The cloud did not affect the SW formation and the criteria.

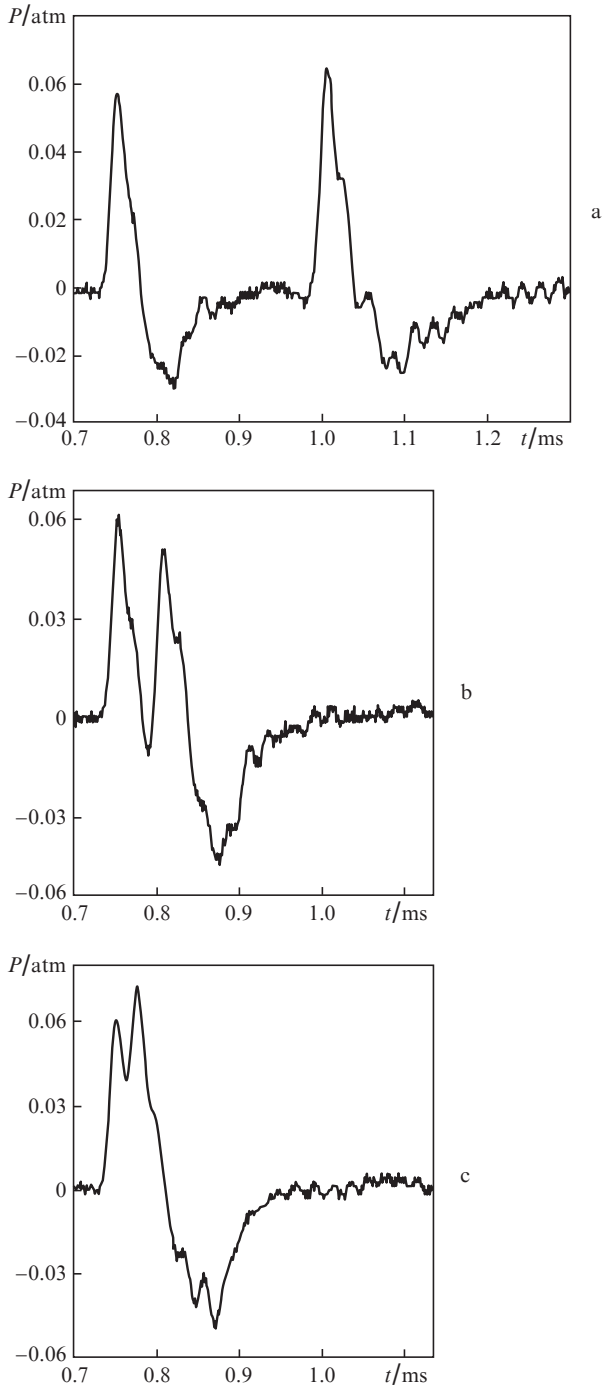

Figure 3. Time dependences of the pressure $P = p - p_0$ in the SWs generated during glass irradiation. The beam areas are $S_1 = 9.5$ cm^2 and $S_2 = 5.5$ cm^2. The varied parameters are (a) $Q_1 = 36$ J, $Q_2 = 35$ J, $t_d = 265$ μs, and $\omega = 1$; (b) $Q_1 = 37$ J, $Q_2 = 35$ J, $t_d = 53$ μs, and $\omega = 5$; and (c) $Q_1 = 37$ J, $Q_2 = 39$ J, $t_d = 38$ μs, and $\omega = 7.3$.

The applicability of the SWM criteria to the irradiation of window glass by laser pulses with a smaller light spot is illustrated in Fig. 3. Here, in contrast to the case shown in Fig. 2, the pulse energy is several times lower, and the energy densities of the first and second pulses differ by a factor of ~2. It can be seen that SWM manifests itself at the same ω values as in the case of Plexiglas irradiation. SW merging depends not only on t_d but also on the pulse energy; this circumstance is taken into account in (2). In particular, at $t_d \approx 35-38$ μs, different energies, and $\omega > 1.5\omega_2$, the front of the second SW comes up with the that of the first SW (Fig. 2c), whereas at smaller ω values the compression phases merge partially (Fig. 3c). The SW and cavity dynamics is shown in the shadow photographs (Fig. 4). The optical breakdowns are localised near the target in a layer thinner than 1 cm. SW becomes hemispherical at $t > 100$ μs. The displacement velocity of cavity boundary decreases, but even at $t \approx 0.5-1$ ms it is as high as ~ 20 m s^{-1}. The bright regions in the cavity are due to the luminescence of hot target vapour.

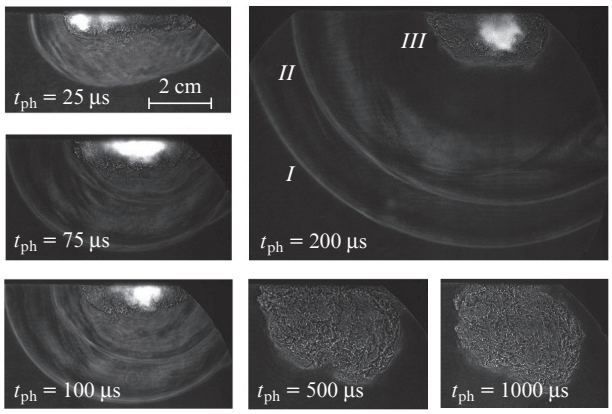

Figure 4. Shadow photographs of the density perturbations formed under irradiation of window glass (correspond to Fig. 3b, $\omega = 4.8$): the fronts of the (*I*) first and (*II*) second SWs and (*III*) the cavity.

Figure 5 shows the SW pressure and the shadow photographs of the perturbations induced by breakdowns on a steel target. An extended plasma plume and breakdown at the aerosol arise at large q values. It can be seen in Fig. 5b that even at an irradiation density of ~ 50 J cm^{-2} a plume that is formed during the first breakdown does not hinder the formation of the second SW. The situation where the front of the second SW comes up with that of the first SW is shown in Fig. 5c. It can be seen in Figs. 5a and 5b, where $t_d = 54$ μs, that the shape and the duration of the compression phase of the merged SW depend on the laser-pulse energy. Note that the irradiated areas are smaller and q is larger (by an order of magnitude) (Fig. 5b) than in the case of Plexiglas irradiation (Fig. 2). The light spots are much smaller in size than R_3 and the distance from the target to the detector R_p; therefore, the breakdown can be considered as a point one. The detector records, first, the sound from the breakdowns at the aerosol (which are located closer) and, second, SWs. Laser pulses induce intense SWs, and SWM is implemented at the same ω values as in the above-considered cases.

Similar experiments were performed for other materials listed above. It is shown that, using expression (1) and the

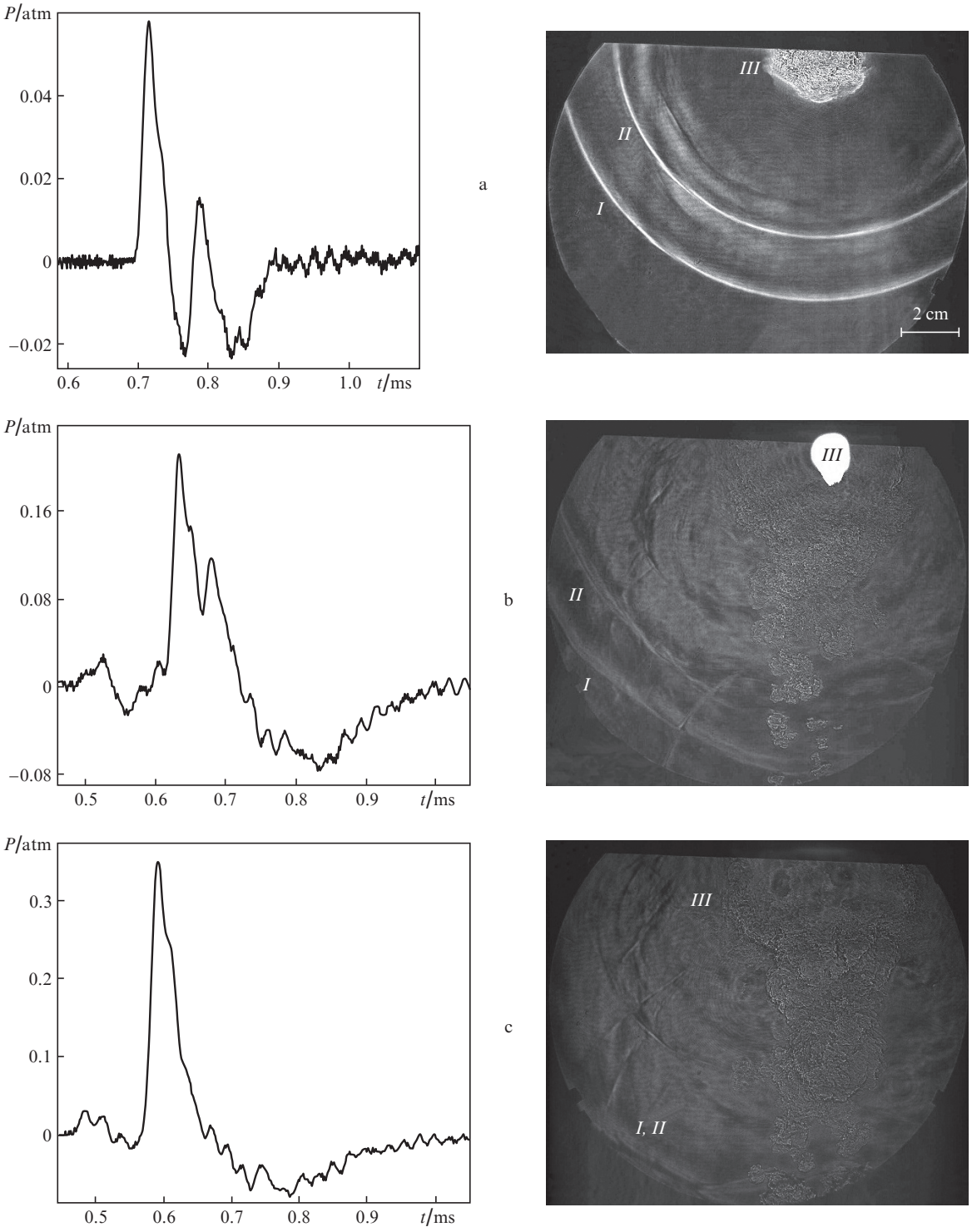

Figure 5. Time dependences of the pressure $P = p - p_0$ in SWs (left) and shadow photographs of the perturbations induced during steel irradiation (right): the fronts of the (*I*) first and (*II*) second SWs and (*III*) the cavity. The beam areas are $S_1 = 4.2$ cm^2 and $S_2 = 2.44$ cm^2. The shadow photographs were made at $t = 200$ μs. The varied parameters are (a) $Q_1 = 28$ J, $Q_2 = 21$ J, $t_d = 54$ μs, and $\omega = 4.2$; (b) $Q_1 = 173$ J, $Q_2 = 117$ J, $t_d = 54$ μs, and $\omega = 7.3$; and (c) $Q_1 = 193$ J, $Q_2 = 131$ J, $t_d = 3$ μs, and $\omega = 156$.

boundary frequencies $\omega_1 \approx 1$ and $\omega_2 \approx 7$, one can estimate the conditions for SWM manifestation. Note that SWM is implemented in different media and for SW sources of different nature. In each particular case it is necessary to refine the SW formation conditions. For example, at $\lambda = 10.6$ and 1.06 μm the optimal q values may differ, which is related to the difference in the breakdown thresholds and, in particular, with the fact that window glass is transparent for light with $\lambda = 1.06$ μm.

Example of using the criteria. Let repetitively pulsed radiation have an average power of W. The frequencies $\omega \approx 4-5$ correspond to ultrasound and intense low-frequency sound. The expressions for the pulse energy and repetition frequency can be found using criteria (2): $Q = 4.4 W^{3/2} c_0^{-3/2} \omega^{-3/2} p_0^{-1/2}$,

$f = 1.41 \times 10^6 \omega^{3/2}/W^{1/2}$ ($p_0 = 1$ atm and $c_0 = 3.4 \times 10^4$ cm s^{-1}). Assuming that $W = 10^5$ W and $\omega = 4$, we obtain $Q = 2.8$ J, $f = 3.6 \times 10^4$ Hz, and $S = Q/q \approx 2.8$ (J)/5 (J cm^{-2}) = 0.56 cm^2.

3. Conclusions

Thus, the criteria of SW merging are applicable to targets made of different materials, exposed to repetitively pulsed laser radiation in a wide range of powers. These criteria make it possible to determine the parameters of repetitively pulsed radiation at which sound with a spectrum containing both ultrasonic and intense low-frequency components can be generated. The range of application of the criteria is limited by the materials absorbing CO_2-laser radiation in a thin surface layer.

Acknowledgements. We are grateful to A.G. Ponomarenko for his support and helpful hints. This study was supported by the Russian Foundation for Basic Research (Project No. 09-08-00830-a).

References

1. Raizer Yu.P. *Lazernaya iskra i rasprostranenie razryadov* (Laser Spark and Propagation of Discharges) (Moscow: Nauka, 1974) p. 308.
2. Prokhorov A.I., Konov V.I., Ursu I., Mihailesku I.N. *Vzaimodeistvie lazernogo izlucheniya s metallami* (Interaction of Laser Radiation with Metals) (Moscow: Nauka, 1988) p. 537.
3. Danilychev V.A., Zvorykin V.D. *Trudy FIAN*, **142**, 117 (1983).
4. Ostrovskaya G.V., Zaidel' A.N. *Usp. Fiz. Nauk*, **11**, 579 (1973).
5. Bunkin F.V., Tribol'skii M.I. *Usp. Fiz. Nauk*, **130** (2), 193 (1980).
6. Lyamshev L.M. *Usp. Fiz. Nauk*, **135** (4), 637 (1981).
7. Geints Yu.E., Zemlyanov A.A., Zuev V.E., Kabanov A.M., Pogodaev V.A. *Nelineinaya optika atmosfernogo aerozolya* (Nonlinear Optics of Atmospheric Aerosol) (Novosibirsk: Izd-vo SO RAN, 1999) p. 259.
8. Tret'yakov P.K., Grachev G.N., Ivanchenko A.I., Krainev V.L., Ponomarenko A.G., Tishchenko V.N. *Dokl. Akad. Nauk.*, **336** (4), 466 (1994).
9. Apollonov V.V., Kiiko V.V., Kislov V.I., Suzdal'tsev A.G., Egorov A.B. *Kvantovaya Elektron.*, **33** (9), 753 (2003) [*Quantum Electron.*, **33** (9), 753 (2003)].
10. Malov A.N., Orishich A.M., Fomin V.M., Vnuchkov D.A., Nalivaichenko D.G., Chirkashenko V.F. *Izv. Tomsk Politekh. Univ.*, **317** (4), 155 (2010).
11. Myrabo L.N., Raizer Yu.P. *AIAA Paper* No. 94-2451 (1994).
12. Tret'yakov P.K., Garanin A.F., Grachev G.N., Krainev V.L., Ponomarenko A.G., Tishchenko V.N. *Dokl. Akad. Nauk.*, **351** (3), 339 (1996).
13. Borzov V.Yu., Mikhailov V.M., Rybka I.V., Yur'ev A.S. *Inzh. Fiz. Zh.*, **66** (5), 515 (1994).
14. Grachev G.N., Tishchenko V.N., Apollonov V.V., Gulidov A.I., Smirnov A.L., Sobolev A.V., Zimin M.I. *Kvantovaya Elektron.*, **37** (7), 669 (2007) [*Quantum Electron.*, **37** (7), 669 (2007)].
15. Bagaev S.N., Grachev G.N., Ponomarenko A.G., Smirnov A.L., Demin V.N., Okotrub A.V., Baklanov A.M., Onishchuk A.A. *Nauka i nanotekhnologii* (*Science and Nanotechnologies*) (Novosibirsk: Izd-vo SO RAN, 1999) p. 123.
16. Tishchenko V.N., Grachev G.N., Zapryagaev V.I., Smirnov A.L., Sobolev A.V. *Kvantovaya Elektron.*, **32** (4), 329 (2002) [*Quantum Electron.*, **32** (4), 329 (2002)].
17. Tishchenko V.N. *Kvantovaya Elektron.*, **33** (9), 823 (2003). [*Quantum Electron.*, **33** (9), 823 (2003)].
18. Tishchenko V.N., Apollonov V.V., Grachev G.N., Gulidov A.I., Zapryagaev V.I., Men'shikov Ya. G., Smirnov A.L., Sobolev A.V. *Kvantovaya Elektron.*, **34** (10), 941 (2004) [*Quantum Electron.*, **34** (10), 941 (2004)].
19. Grachev G.N., Ponomarenko A.G., Tishchenko V.N., Smirnov A.L., Trashkeev S.I., Statsenko P.A., Zimin M.I., et al. *Kvantovaya Elektron.*, **36** (5), 470 (2006) [*Quantum Electron.*, **36** (5), 470 (2006)].
20. Grachev G.N., Ponomarenko A.G., Smirnov A.L., Statsenko P.A., Tishchenko V.N., Trashkeev S.I. *Kvantovaya Elektron.*, **35** (11), 973 (2005) [*Quantum Electron.*, **35** (11), 973 (2005)].
21. Tishchenko V.N., Grachev G.N., Pavlov A.A., Smirnov A.L., Pavlov Al.A., Golubev M.P. *Kvantovaya Elektron.*, **38** (1), 82 (2008) [*Quantum Electron.*, **38** (1), 82 (2008)].
22. Yakovlev Yu.S. *Gidrodinamika vzryva* (*Explosion Hydrodynamics*) (Leningrad.: Sudpromgiz, 1961) p. 313.
23. Tishchenko V.N., Shaikhislamov I.F. *Kvantovaya Elektron.*, **40** (5), 464 (2010) [*Quantum Electron.*, **40** (5), 464 (2010)].
24. Orishich A.M., Ponomarenko A.G., Posukh V.G. *Zh. Prikl. Mekh. Teor. Fiz.*, (2), 27 (1987).
25. Tishchenko V.N., Ponomarenko A.G., Posukh V.G., Pavlov A.A., Zapryagaev V.I., et al. *Sb. trudov XX sessii Rossiiskogo akusticheskogo obshchestva* (Proceedings of the XX Session of the Russian Acoustic Society) (Moscow: GEOS, 2008) p. 112.